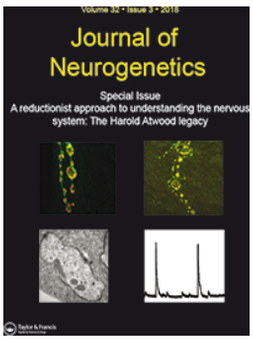

Taylor & Francis
Taylor & Francis Group

Journal of Neurogenetics

ISSN: 0167-7063 (Print) 1563-5260 (Online) Journal homepage: https://www.tandfonline.com/loi/ineg20

Pleiotropy of the *Drosophila melanogaster foraging* gene on larval feeding-related traits

A. M. Allen, I. Anreiter, A. Vesterberg, S. J. Douglas & M. B. Sokolowski

To cite this article: A. M. Allen, I. Anreiter, A. Vesterberg, S. J. Douglas & M. B. Sokolowski (2018) Pleiotropy of the *Drosophila melanogaster foraging* gene on larval feeding-related traits, Journal of Neurogenetics, 32:3, 256-266, DOI: 10.1080/01677063.2018.1500572

To link to this article: https://doi.org/10.1080/01677063.2018.1500572

JOURNAL OF NEUROGENETICS
2018, VOL. 32, NO. 3, 256–266
https://doi.org/10.1080/01677063.2018.1500572

Taylor & Francis
Taylor & Francis Group

ORIGINAL RESEARCH ARTICLE

Pleiotropy of the *Drosophila melanogaster foraging* gene on larval feeding-related traits

A. M. Allen[a]†, I. Anreiter[b,c], A. Vesterberg[b], S. J. Douglas[a] and M. B. Sokolowski[a,b,c]

[a]Department of Cell and Systems Biology, University of Toronto, Toronto, Canada; [b]Department of Ecology and Evolutionary Biology, University of Toronto, Toronto, Canada; [c]Child and Brain Development Program Canadian Institute for Advanced Research (CIFAR) MaRS Centre, Toronto, Canada

ABSTRACT

Little is known about the molecular underpinning of behavioral pleiotropy. The *Drosophila melanogaster foraging* gene is highly pleiotropic, affecting many independent larval and adult phenotypes. Included in *foraging's* multiple phenotypes are larval foraging path length, triglyceride levels, and food intake. *foraging* has a complex structure with four promoters and 21 transcripts that encode nine protein isoforms of a cGMP dependent protein kinase (PKG). We examined if *foraging*'s complex molecular structure underlies the behavioral pleiotropy associated with this gene. Using a promotor analysis strategy, we cloned DNA fragments upstream of each of *foraging*'s transcription start sites and generated four separate for^{pr}-*Gal4*s. Supporting our hypothesis of modular function, they had discrete, restricted expression patterns throughout the larva. In the CNS, for^{pr1}-*Gal4* and for^{pr4}-*Gal4* were expressed in neurons while for^{pr2}-*Gal4* and for^{pr3}-*Gal4* were expressed in glia cells. In the gastric system, for^{pr1}-*Gal4* and for^{pr3}-*Gal4* were expressed in enteroendocrine cells of the midgut while for^{pr2}-*Gal4* was expressed in the stem cells of the midgut. for^{pr3}-*Gal4* was expressed in the midgut enterocytes, and midgut and hindgut visceral muscle. for^{pr4}-*Gal4*'s gastric system expression was restricted to the hindgut. We also found promoter specific expression in the larval fat body, salivary glands, and body muscle. The modularity of *foraging*'s molecular structure was also apparent in the phenotypic rescues. We rescued larval path length, triglyceride levels (bordered on significance), and food intake of for^{0} null larvae using different for^{pr}-*Gal4*s to drive *UAS-*for^{cDNA}. In a *foraging* null genetic background, for^{pr1}-*Gal4* was the only promoter driven Gal4 to rescue larval path length, for^{pr3}-*Gal4* altered triglyceride levels, and for^{pr4}-*Gal4* rescued food intake. Our results refine the spatial expression responsible for *foraging*'s associated phenotypes, as well as the sub-regions of the locus responsible for their expression. *foraging*'s pleiotropy arises at least in part from the individual contributions of its four promoters.

ARTICLE HISTORY
Received 16 May 2018
Accepted 9 July 2018

KEYWORDS
Drosophila melanogaster; *foraging* gene; pleiotropy; multiple promoter analysis; larval phenotypes

Introduction

Genes that regulate behavior, with their often complex molecular structures, are fertile ground for investigations into the molecular basis of pleiotropy. One such gene is the *foraging* gene of *Drosophila melanogaster* which encodes a cGMP dependent protein kinase (PKG). *foraging* has four promoters, 21 transcripts, and nine open reading frames (Allen, Anreiter, Neville, & Sokolowski, 2017; Kalderon & Rubin, 1989) all of which share a common protein kinase domain. This pleiotropic complex gene is known to play a role in multiple larval and adult behavioral phenotypes (Reaume & Sokolowski, 2011). The best studied of these are the larval feeding-related traits: larval foraging path length, triglyceride levels, and food intake (Allen *et al.*, 2017; Kaun *et al.*, 2007; Osborne *et al.*, 1997). These phenotypes reflect the larva's ability to navigate its environment, ingest food, and store the resources for times of need, all of which are important for larval survival to adulthood.

There are many ways that molecularly complex genes can accomplish their pleiotropic effects (Hodgkin, 1998; Pyeritz, 1989). Below are examples of how pleiotropy can be accomplished at the molecular level. These examples are not mutually exclusive. In the first example, the multiple transcripts that produce distinct protein products differ in their downstream targets. In the case of *foraging*, all of its 21 transcripts code for the same kinase domain but they differ in their regulatory domains (Allen *et al.*, 2017; Kalderon & Rubin, 1989; Osborne *et al.*, 1997). *foraging*'s mammalian orthologue, *cGKI*, produces multiple isoforms with differing expression, biochemical activity, and interacting partners and substrates (Hofmann, Bernhard, Lukowski, & Weinmeister, 2009; Schlossmann & Desch, 2009; Smith, Francis, Walsh, Kumar, & Corbin, 1996). In the second example, the cellular environment as well as the spatial and temporal expression pattern can affect post-transcriptional regulation. *foraging* is known

CONTACT M. B. Sokolowski marla.sokolowski@utoronto.ca Department of Cell and Systems Biology, University of Toronto, 25 Harbord Street, Toronto, ON, Canada M5S 3G5
†Current address: Centre for Neural Circuits and Behaviour, University of Oxford, Oxford, OX1 3SR, UK

Supplemental data for this article can be accessed here.

to be expressed in many different tissue systems (Chintapalli, Wang, & Dow, 2007; Graveley *et al.*, 2011). In the third example, a gene's multiple promoters are regulated independently; they drive gene products during different times in development, in different tissues and/or in response to distinctive environmental stimuli. This likely arises from differences in the transcription factor binding sites found in each of the promoter specific sequences (Anreiter, Kramer, & Sokolowski, 2017; Anreiter & Sokolowski, 2018). As with the *D. melanogaster foraging* gene, the use of alternative promoters that result in mRNA transcripts with different 5′-untranslated regions is a regularly used mechanism in eukaryotes to ensure the proper level of expression, timing, and cell specificity of a gene (Ayoubi & Van De Ven, 1996). Variations within *cis*-regulatory elements, the regions of DNA bound by transcription factors, can also affect a subset of the spatial- or temporal-expression of the gene. These regulatory differences are known to be important for morphological, physiological, and behavioral evolution between lineages (Andersson & Georges, 2004; Carroll, 2000; Hofmann, 2003).

Allen *et al.* (2017) experimentally defined *foraging's* transcription start sites, termination sites, and splicing patterns utilizing rapid amplification of cDNA ends (RACE) and full-length cDNA sequencing. As mentioned above, this uncovered four independent promoters *pr1–4*, that produce 21 transcripts with nine distinct open reading frames. The authors postulated that the use of alternative promoters and splicing at this locus can generate diversity and flexibility in the regulation of gene expression and function. They also generated a null allele (for^0) using homologous recombination to precisely delete *foraging*; recombineering was used to reintegrate a full genomic copy into the genome in increasing doses of the gene to rescue the (for^0) phenotypes. They found that a total loss of *foraging* expression in larvae resulted in reduced larval foraging path length, reduced food intake, and an increase in triglyceride levels (Allen *et al.*, 2017). Their results proved that these larval phenotypes were influenced by *foraging* and suggested that they may be independently regulated from within the locus (Allen *et al.*, 2017).

The independent roles of *foraging*'s promoters in regulating behavior were recently demonstrated in a study on the 'rover', for^R and 'sitter', for^s *foraging* allelic variants, which differ in a variety of *foraging*-related traits (Anreiter *et al.*, 2017). Sitter adults have lower foraging scores, finding and feeding on fewer food drops than rovers. This difference in adult feeding behavior was mediated by the histone methyl transferase *G9a*, which methylates the *foraging* promoters (Anreiter *et al.*, 2017). Sitters had lower G9a-mediated methylation at promoter 4 and higher expression of promoter 4 transcripts. Decreasing promoter 4 expression in sitters with a transcript-specific RNAi transformed sitter feeding behavior into a rover (Anreiter *et al.*, 2017). These findings further supported the hypothesis that the four promoters of *foraging* are independently regulated to affect distinct phenotypes.

Here, we propose that *foraging* achieves its pleiotropy through its complex molecular structure and that separate regulatory regions along the locus drive expression of the promoters in a tissue-specific manner. We begin with a promoter analysis approach, employing the *Gal4/UAS* system (Brand & Perrimon, 1993). This approach was successfully used to identify a gene's regulatory regions and deduce expression and function (Arredondo *et al.*, 2001; Billeter & Goodwin, 2004; Brenner et al 1996; Lehman *et al.*, 1999; Okada *et al.*, 2001; Park *et al.*, 2000; Thomas, Wang, Brenner, & Atkinson, 1997). We generated four promoter-*Gal4* fusions (for^{pr}-*Gal4*) 5′ to each of the four *foraging* transcription start sites and then characterized their expression patterns in larvae using a green fluorescent protein (GFP) reporter (Lee & Luo, 1999; Ormö *et al.*, 1996). To rescue the effects of the for^0 null mutant allele on larval path length behavior, triglyceride levels, and food intake, we drove a *UAS-*for^{cDNA} with each of the newly generated four for^{pr}-*Gal4*s in a for^0 background and measured the effects on these larval phenotypes. We found that: (1) each for^{pr}-*Gal4* expressed in many tissue systems, including the nervous system, gastric system, as well as other various tissues including fat body and muscle and, (2) expression from different *foraging* promoters rescued distinct larval phenotypes of *foraging* null larvae. We concluded that *foraging*'s complex modular structure allows for independent regulation and expression of *foraging*'s larval phenotypes.

Materials and methods

Strains and rearing

Strains were kept in 40 ml vials containing 10 ml of cornmeal/molasses fly food (described in Allen *et al.*, 2017) or 170 ml bottles with 40 ml of the same fly food. Flies were reared at 25 ± 1 °C with a 12L:12D photocycle with lights on at 0800 h. Third instar larvae were developmentally synchronization as in Anreiter, Vasquez, Allen, and Sokolowski (2016). Briefly, 5- to 7-day-old adults laid eggs on a grape juice and agar media. After 20 h, early hatched larvae were removed and discarded. The plates were incubated for 4 h and newly hatched larvae were placed into Petri dishes containing fly food. Larvae were incubated for 3 days until they reached mid third instar (72 ± 2 h post-hatch).

The *UAS foraging cDNA* (also called UAS-T1 in Belay *et al.*, 2007) was made from cDNA encoded by the gene's RNA transcript A (RA; see Allen *et al.*, 2017). It is shown in Figure 1 and was previously generated in the laboratory of M. B. Sokolowski (University of Toronto). *UAS-Stinger* (Barolo, Carver, & Posakony, 2000) was obtained from J. D. Levine (University of Toronto). *UAS-mCD8::GFP* was from the Bloomington Drosophila Stock Center. The for^0 allele is described in Allen *et al.* (2017). All behavioral and metabolic phenotypes were conducted on strains that were backcrossed for nine generations into the for^s genetic background. The more recently isogenized for^s and for^R strains described in Anreiter *et al.* (2017) were used as additional controls for the phenotyping experiments. The rover strain, isogenized in the late 1990's, and described in Kaun et al., (2007) was used to generate the *forpr-Gal4* transgenes.

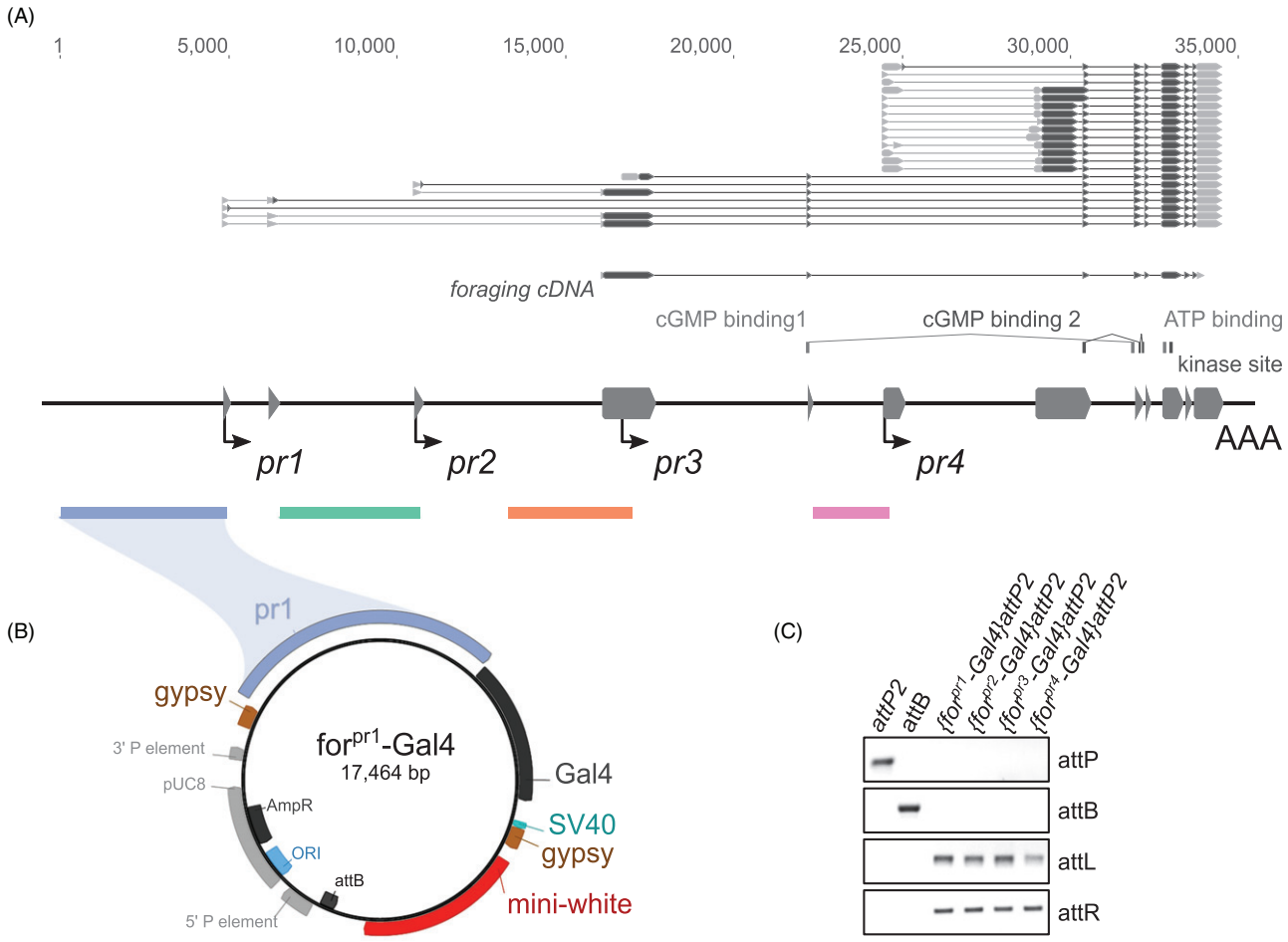

Figure 1. Cloning of *for*^{pr}*-Gal4*s. (A) Schematic of the *foraging* locus (dark grey – exons), its transcripts above the locus (grey – UTR, black – ORF), transcription start sites (arrows) and the cloned regions (colored bars below locus) used in the promoter analysis. The regions up to 5 kb upstream of and 300 bp downstream of the TSS for the four identified minimal promoters were cloned into a *gypsy* insulated *Gal4* vector. The ORF used in the *UAS-for*^{cDNA} is annotated below the transcripts and is a derivative of the RNA transcript A (RA) and codes for the protein isoform A (PA). (B) Example of one of the cloned *for*^{pr1}*-Gal4* constructs. The *for*^{pr1}*-Gal4* segment is flanked by *gypsy* insulator sequences. An *attB* site-specific recombination sequence from φC31 was added to the vector. (C) PCR confirmation of the four *for*^{pr}*-Gal4* integrations. There was a positive integration event in all lines.

Promoter-Gal4s

Bioinformatics were conducted with the Geneious software package (Kearse *et al.*, 2012). An *attB* sequence was amplified with PCR from the pUAST-*attB* vector (Bischof, Maeda, Hediger, Karch, & Basler, 2007).

(attB-F: ATGCATGTCTGGATCCACTAGTGTCG,
attB-R: ATGCATGCTGGCTAGAACTAGTGTCG).

*Nsi*I sites were added to the primers. The *Nsi*I fragment was then cloned into the pStinger vector (Barolo *et al.*, 2000). Regions of the *foraging* gene were amplified with PCR and cloned into pGEM-Teasy vector (Promega, Madison, WI, USA).

(forpr1Gal4-F: GAGCTCTCCGCAGTCCCTATTCTTCCC,
forpr1Gal4-R: GGTACCACAAGTCGATGAAAAACCGCC,
forpr2Gal4-F: GAGCTCGTAAGCTCCATTTTAATATGC,
forpr2Gal4-R: GGTACCCCAAAACCAAGTGTAACACAC,
forpr3Gal4-F: GAGCTCAAGGATGCAAGATGTCTG,
forpr3Gal4-R: GGTACCGGGATCCTGGTTCAATTGCTG,
forpr4Gal4-F: GAGCTCGTGAGTTGAAGCTCCAAGC,
forpr4Gal4-R: GGTACCCGAATTGAAAATCACGATACG).

Each region included its respective transcription-start-site and extended 5′ to varying lengths. The total fragment sizes were; *pr1*–4.9 kb, *pr2*–4.2 kb, *pr3*–3.7 kb, *pr4*–2.3 kb. *Sac*I sites were added to the forward primers and *Kpn*I sites were added to the reverse primers (underlined). The *Sac*I/*Kpn*I fragments were digested out of pGEM and inserted into the Gal4 containing pMARTINI-*Gal4* vector (Billeter & Goodwin, 2004). The *Not*I *pr-Gal4* fragments were then inserted into the pStinger-*attB* vector, replacing the *eGFP* sequence. The resulting vector contained a *pr-Gal4* sequence between two gypsy insulators with an *attB* sequence. All *for*^{pr}*-Gal4* constructs were injected into the *P{CaryP}attP2* landing site (Groth, Fish, Nusse, & Calos, 2004) by Genetic Services Inc. Successful integration was confirmed with PCR. The *P{CaryP}attP2* integration site was chosen for its high levels of inducible expression and low levels of leaky expression from position effects (Groth *et al.*, 2004; Markstein, Pitsouli, Villalta, Celniker, & Perrimon, 2008). The cloning of the four *for*^{pr}*-Gal4* lines is shown in Figure 1 along with a schematic of the *foraging* gene.

Whole-mount immunofluorescence

Dissected samples were fixed in 4% paraformaldehyde in 1× PBS for 1 h. The fixed samples were rinsed twice in 0.5% Triton X in one time PBS (PBT) and then washed four

times for 30 min each in PBT. The samples were blocked in 10% normal goat serum (NGS, Jackson ImmunoResearch Laboratories, West Grove, Pennsylvania, USA) and 0.1% BSA (Sigma, St. Louis, MO, USA) in PBT for 2 h at room temperature. Primary antibody incubations (Rabbit anti-GFP, 1:600, Thermo Fisher, Waltham, MA, USA, cat#A-11122) were conducted in blocking solution and incubated overnight at 4 °C. After primary incubation the samples were rinsed twice and then washed four times for 30 min each in PBT. Secondary antibody (Alexa Fluor 488, goat anti-Rabbit IgG, 1:2000, Thermo Fisher cat#A-11034) was incubated in PBT at room temperature for 2 h. Washing was conducted as described above for the primary antibody. Tissues were mounted on slides in Vectashield (Vector Labs, Burlingame, CA, USA). Samples were imaged using a Zeiss LSM 510 and Leica SP5 confocal microscopes. Images were analysed using Fiji software package (Schindelin *et al.*, 2012). Dissection was done under a *GFP* dissection scope so that the entire larva could be examined for *GFP* expression. Subsequently, the CNS, guts, fat bodies, salivary glands, and carcasses were stained and mounted on slides and imaged on the confocal. The expression reported here represents what was consistent between endogenous fluorescence and antibody staining for both an *mCD8::GFP* and a nls::*GFP*. Imaging was performed on fly strains with both the original genetic backgrounds, post injection, as well as on strains backcrossed for 9 generations into the for^{s} background; no genetic background effects were found.

Path length

The larval path length protocol is detailed in Anreiter *et al.* (2016). Briefly, mid-third instar larvae (72 ± 2 h post-hatch) were removed from food plates and rinsed in water. A yeast paste solution (2:1 w/w) was spread across the wells of custom black rectangular Plexiglas plates, creating a thin even layer of yeast paste in each well. Larvae were placed in each well and covered with a Petri dish lid. After 5 min the path lengths left in the yeast paste were traced onto the Petri dish lid. Path lengths were digitized using Fiji (Schindelin *et al.*, 2012). Because of the extent of the larval path length assays, rescue experiments for the *pr-Gal4* lines had to be tested on different days. Consequently, additional for^{R} and for^{s} controls were run for the path length experiments. Data are shown in Figure S2.

Food intake

Larval food intake assays were performed as described in Allen *et al.* (2017). Briefly, larvae were place in tissue culture dishes with liquid food contained 0.5% fluorescein, 5% sucrose, and 5% yeast extract. Larvae were left to feed for 10 min, washed three times in water, and placed into a 1.5 ml tube and frozen. Groups of 10 larvae were homogenized in 1× PBS and then centrifuged. The supernatant was analyzed with a fluorometer. Larvae that were fed food without fluorescein were homogenized and used as a blank.

Triglyceride analysis

Triglyceride analysis was performed as described in Allen *et al.* (2017). Briefly, groups of 10 larvae were homogenized in 200 µl of 0.1% Tween 20 in 1× PBS. Homogenates were incubated at 70 °C for 5 min and then incubated on ice for 2 min prior to centrifugation. A small aliquot of the supernatant was analyzed with Infinity TAG Reagent (Thermo Scientific, Waltham, MA, USA, cat# TR22421) following manufacturers specifications. A separate aliquot was analyzed with Pierce BCA Protein Assay Kit (Thermo Scientific, cat# 23227) to quantify protein levels in the samples following manufacturers' specifications. Triglyceride levels are displayed as µg glycerol/mg protein.

Statistical analysis and data availability

Statistical analysis was performed in R (R Core Team, 2013). ANOVA and Tukey HSD *post hoc* tests were run to compute statistical significances and are summarized in Supplementary Table 1. The boxplots show the mean with the whiskers displaying 1.5 times the interquartile range. For a rescue to be considered significant the *UAS/Gal4* treatment had to be significantly different than both of the *UAS* and the *Gal4* controls. Plots were edited with Inkscape. All data are available upon request.

Results

Figure 1(A) shows a schematic of the *foraging* gene showing each of its four promoters and the DNA fragments cloned 5′ to each fragment. *foraging's* RNA transcripts along with the *foraging* cDNA used in this study are shown at the top of the figure. Figure 1(B) shows how the for^{pr1}-*Gal4* constructs were cloned and Figure 1(C) shows that each of the constructs was integrated in all the for^{pr1}-*Gal4* lines.

for^{Pr}-Gal4 expression

Each of the four for^{pr}-*Gal4* lines showed expression in varying cell types in different tissue systems in larvae (Figure 2, Figure S1). All four promoters expressed in the CNS, each having a distinct, non-overlapping cellular expression pattern (Figure 2). for^{pr1}-*Gal4* and for^{pr4}-*Gal4* were expressed in neurons, while for^{pr2}-*Gal4* and for^{pr3}-*Gal4* were expressed in glia, but not neurons. for^{pr1}-*Gal4* expressed in neurons throughout the central brain and VNC (Figure 2(B)), whereas for^{pr4}-*Gal4* expression was restricted primarily to the optic lobes, the eye imaginal discs, and the leg imaginal discs (Figure 2(E)). for^{pr2}-*Gal4* expressed in the midline glia (Figure 2(C)). for^{pr3}-*Gal4* expressed in the surface glia (Figure 2(D)).

Similarly, all for^{pr}-*Gal4*s were expressed in the gut but each in a different set of cells (Figure 3). Expression of for^{pr1}-*Gal4* was evident in a few enteroendocrine cells (EEC) in the anterior of the midgut (Figure 2(F)). for^{pr2}-*Gal4* was expressed in the adult midgut precursors (AMPs), which include the intestinal stem cells (Figure 2(G), Figure S1(B)).

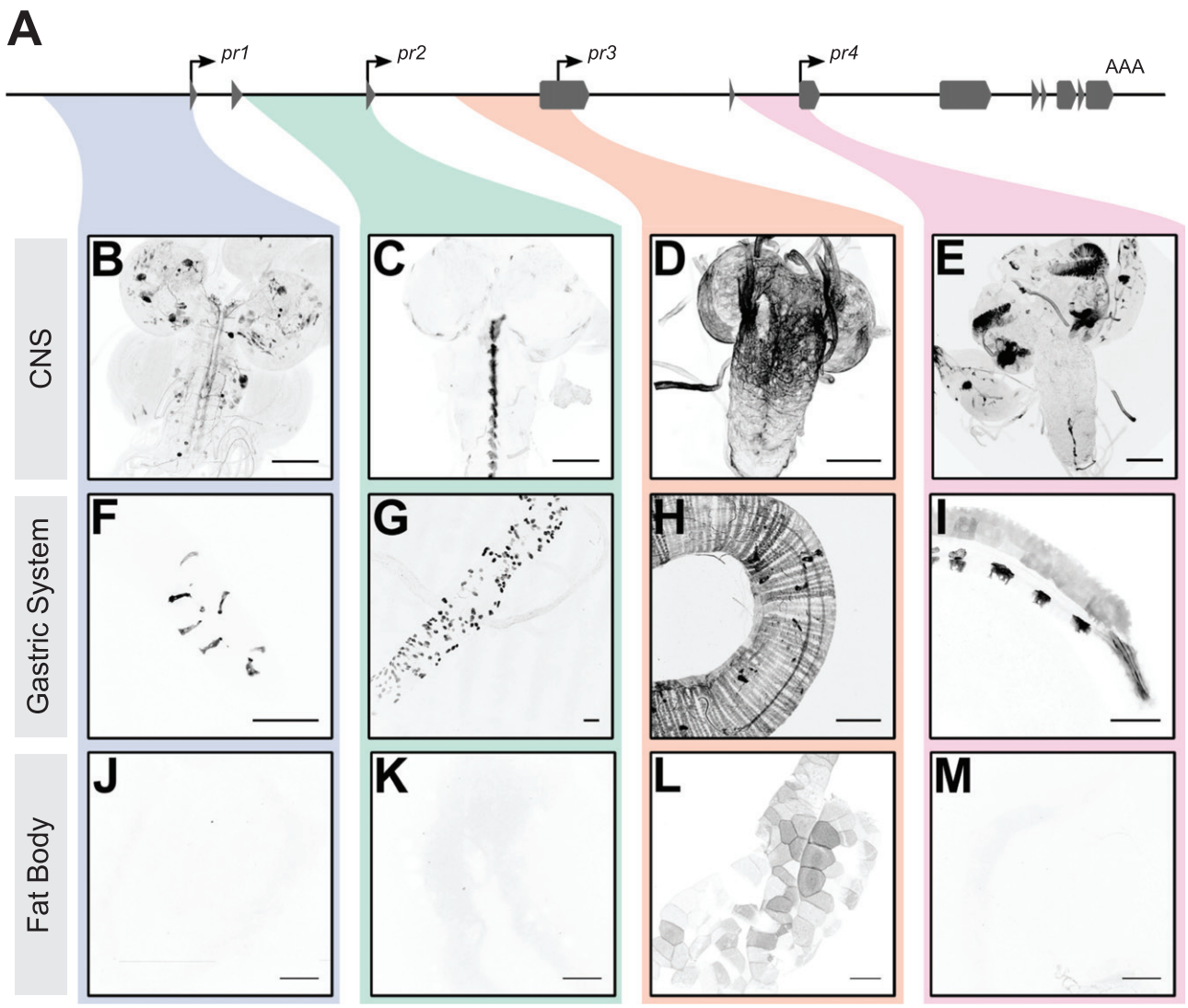

Figure 2. *for^{pr}-Gal4s* expression in the 3rd instar larval CNS, gastric system, and fat body. Whole-mount immunofluorescence analysis of *for^{pr}-Gal4* driving *UAS-mCD8::GFP* in the larval CNS and stained with anti-GFP. Sample sizes were $n \geq 12$ larvae for each of experiment. Representative images are shown. Scale bars = 100 μm. (A) Schematic of the *foraging* locus with the cloned regions near the transcription start sites highlighted. (B) *for^{pr1}-Gal4* expressed in neurons throughout the VNC and brain lobes. (C) *for^{pr2}-Gal4* expressed in midline glia in the VNC. (D) *for^{pr3}-Gal4* expressed in the perineurial surface glia of the CNS and PNS. (E) *for^{pr4}-Gal4* expressed in the optic lobes of the CNS and the eye imaginal discs and the leg imaginal discs. (F) *for^{pr1}-Gal4* expressed in enteroendocrine cells in the anterior portion of the larval midgut. (G) *for^{pr2}-Gal4* expressed in the adult midgut precursor cells (AMP) throughout the midgut. (H) *for^{pr3}-Gal4* expressed in the muscle of the midgut. (I) *for^{pr4}-Gal4* expressed in the h5d, h6d, hv, and h7 regions of the larval hindgut. (J) *for^{pr1}-Gal4* was not expressed in fat body. (K) *for^{pr2}-Gal4* was not expressed in fat body. (L) *for^{pr3}-Gal4* was expressed in the fat body. (M) *for^{pr4}-Gal4* was not expressed in fat body.

for^{pr2}-Gal4 also expressed in the ureter of the Malpighian tubules (data not shown). *for^{pr3}-Gal4* had the broadest expression of the four drivers in the gastric system. *for^{pr3}-Gal4* expressed in midgut anterior enterocytes (Figure 3(H)), the copper cells responsible for acid secretion (Dubreuil, 2004), as well as the large flat cells of the middle midgut, important for the secretion and absorption. *for^{pr3}-Gal4* also drove expression in the circular and longitudinal muscle of the midgut and hindgut (Figure 2(H), Figure S1(E)) necessary for peristaltic contraction in the gastric system. Additionally, *for^{pr3}-Gal4* expressed in EEC further down the midgut from *for^{pr1}-Gal4* (Figure 2(H), Figure S1(F)). Finally, *for^{pr3}-Gal4* expressed in the primary cells of the anterior Malpighian tubules (Figure S1(H)). *for^{pr4}-Gal4* expressed exclusively in the hindgut (Figure 2(I)). The larval hindgut is separated into many distinct sections, each with differing functions. *for^{pr4}-Gal4* expressed in the h3 (peristaltic contractions), h5d and h6d (ion and water transport), hv (absorption), and h7 (contractions for fecal waste) regions of the hindgut (Figure 2(I), Figure S1(O)) (Murakami & Shiotsuki, 2001).

Finally, both *for^{pr2}-Gal4* and *for^{pr4}-Gal4* expressed in the salivary gland imaginal ring (Figure S1(C, N)), which develops into the adult salivary duct and gland during metamorphosis. *for^{pr3}-Gal4* expressed in the developed larval salivary gland (Figure S1(I)) and extensively in body wall muscle (Figure S1(D)). *for^{pr3}-Gal4* expressed in the fat body (Figure 2(L)). In contrast, *for^{pr1}-Gal4*, *for^{p2}-Gal4*, and *for^{p4}-Gal4* did not expressed in the fat body (Figure 2(J, K, M), respectively). *for^{pr4}-Gal4* expressed in dorsal denticles (Figure S1(K)), as well as the anterior and posterior spiracles (Figure S1(L,M)). Although the four *for^{pr}-Gal4s* show broad expression, with *for^{pr3}-Gal4* being the broadest, their expression patterns are striking in their cell and tissue specificity.

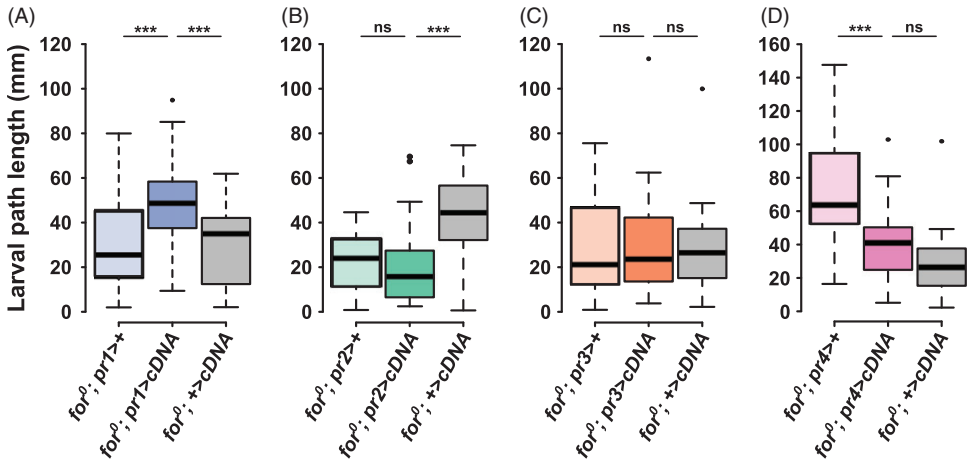

Figure 3. *for^{pr1}-Gal4* rescues *foraging* null (*for^{0}*) larval path length. (A) The *pr1* experimental (*for^{0}/for^{0}; {for^{pr1}-Gal4}/{UAS-for^{cDNA}}*) had significantly longer path lengths than either the *Gal4* control (*for^{0}/for^{0}; {for^{pr1}-Gal4}/+*, $p = .00041$) and the *UAS* control (*for^{0}/for^{0}; +/{UAS-for^{cDNA}}*, $p = .0004$). (B) The *pr2* experimental (*for^{0}/for^{0}; {for^{pr2}-Gal4}/{UAS-for^{cDNA}}*) did not have significantly longer path lengths than the *Gal4* control (*for^{0}/for^{0}; {for^{pr2}-Gal4}/+*, $p = .95$). (C) The *pr3* experimental (*for^{0}/for^{0}; {for^{pr3}-Gal4}/{UAS-for^{cDNA}}*) was not significantly different from the *Gal4* control (*for^{0}/for^{0}; {for^{pr3}-Gal4}/+*, $p = .93$) or the *UAS* control (*for^{0}/for^{0}; +/{UAS-for^{cDNA}}*, $p = .89$). (D) The *pr4* experimental (*for^{0}/for^{0}; {for^{pr4}-Gal4}/{UAS-for^{cDNA}}*) was not significantly different from the *UAS* control (*for^{0}/for^{0}; +/{UAS-for^{cDNA}}*, $p = .17$). Sample size: $n = 30$ larvae per genotype per plot. The boxplots show the mean with the whiskers displaying 1.5 times the interquartile range. For a rescue to be considered significant the *UAS/Gal4* treatment had to be significantly different than both of the *UAS* and the *Gal4* controls.

Modularity of for*'s phenotypic effects*

Above we show that the fragments cloned 5′ to each of *foraging's* promoters drive independent and diverse expression patterns. Next, we determined if expressing *UAS-for^{cDNA}* in each of the *for^{pr}-Gal4*s patterns could significantly change the larval path length, triglyceride levels, and food intake of *for^{0}* null larvae. As is common practice in *Drosophila* research, a transgenic rescue was significant when the *UAS/Gal4* treatment was significantly different than both of the *UAS* and the *Gal4* controls (Figures 3–5). *for^{R}* and *for^{s}* data were collected as additional controls for the *for^{pr}-Gal4* experiments (Figure S2). Here, we determine whether *foraging*'s modular structure with its four promoters, explain the pleiotropic effects of *foraging* on these larval traits.

pr1 > cDNA *increases* for^{0} *path length behavior*

When *foraging* cDNA was expressed using *for^{pr1}-Gal4* the path length of *for^{0}* larvae was significantly higher than the *UAS* or *Gal4* controls ($F_{(2,87)} = 10.7$, $p = 7.2e-05$; treatment compared to *Gal4* control, $p < .001$ and *UAS* control, $p < .001$; Figure 3(A)). This rescue was specific to the *for^{pr1}-Gal4*, as the other three *for^{pr}-Gal4*s did not rescue the path length phenotype (Figure 3(B–D); Table S1). This shows that the *for^{pr1}-Gal4* pattern of expression was specifically needed for altering *for^{0}* larval path length.

pr3 > cDNA *increases* for^{0} *triglyceride levels*

When a *foraging* cDNA was expressed using *for^{pr3}-Gal4* the triglyceride levels of *for^{0}* larvae bordered on being significantly higher than the controls ($F_{(2,27)} = 3.76$, $p = .036$; treatment compared to *Gal4* control, $p < .06$ and *UAS* control, $p < .06$; Figure 4(C)). This border line triglyceride rescue was specific to *for^{pr3}-Gal4* and not the other three *for^{pr}-Gal4*s (Figure 4(A, B, D); Table S1). This suggests that the *for^{pr3}-Gal4* pattern of expression was likely needed for altering *for^{0}* larval triglyceride levels.

pr4 > cDNA *increases* for^{0} *food intake behavior*

When a *foraging* cDNA was expressed using *for^{pr4}-Gal4* the food intake of *for^{0}* larvae was significantly higher than the controls ($F_{(2,27)} = 13.9$, $p = 7.1e-05$; treatment compared to *Gal4* control, $p < .0001$ and *UAS* control, $p < .01$; Figure 5(D)). This rescue was specific to the *for^{pr4}-Gal4* as the other three *for^{pr}-Gal4*s did not rescue the food intake phenotype (Figure 5(A–C); Table S1). This suggests that the *for^{pr4}-Gal4* pattern of expression was specifically needed for altering *for^{0}* larval food intake.

Discussion

Our findings support the hypothesis that *foraging's* modular molecular structure contributes to its pleiotropy (Figure 6). To address this hypothesis, we cloned four regions upstream of the four independent transcription start sites (called *pr1–4)* in the *foraging* gene. We used a GFP reporter to drive the expression of each fragment using *Gal4* and found that each of these clone regions drove independent diverse expression in multiple tissue systems of the larva. *foraging* cDNA expressed using each of the *pr-Gal4* drivers individually rescued foraging path length, triglyceride levels, and food intake of *foraging* null mutant larvae.*for^{pr1}-Gal4* expression was sufficient to rescue the *for^{0}* path length phenotype. *for^{pr1}-Gal4* was found in neurons in the central brain VNC, PNS, and a few enteroendocrine cells in the anterior of the midgut. The release of endocrine molecules from EECs plays a role in maintaining gut homeostasis by sending hormonal cues to the enterocytes to regulate digestion and absorption (Veenstra, 2009). Future research will identify which of these cells in the nervous system and or gut are important for larval foraging path length. *for^{pr2}-Gal4* expression did not

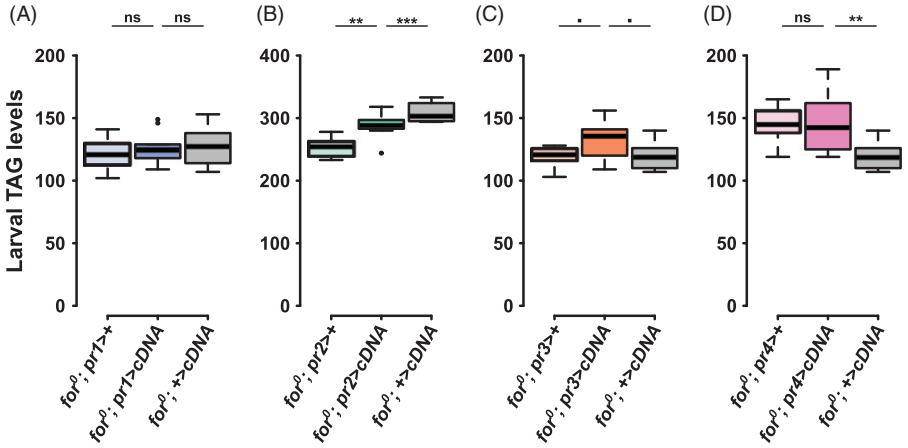

Figure 4. *for^{p3}-Gal4* affects larval triglyceride levels. (A) The *pr1* experimental (*for^{0}/for^{0}; {for^{pr1}-Gal4}/{UAS-for^{cDNA}}*) was not significantly different from the *Gal4* control (*for^{0}/for^{0}; {for^{pr1}-Gal4}/+*, $p = .78$) or the *UAS* control (*for^{0}/for^{0}; +/{UAS-for^{cDNA}}*, $p = 0.94$). (B) The *pr2* experimental (*for^{0}/for^{0}; {for^{pr2}-Gal4}/{UAS-for^{cDNA}}*) was intermediate between the significantly different *Gal4* (*for^{0}/for^{0}; {for^{pr2}-Gal4}/+*) and *UAS* (*for^{0}/for^{0}; +/{UAS-for^{cDNA}}*) controls. (C) There was significant variation in the *pr3* triglyceride experiment ($F_{(2,27)} = 3.76$, $p = .036$). The *pr3* experimental (*for^{0}/for^{0}; {for^{pr3}-Gal4}/{UAS-for^{cDNA}}*) bordered on being significantly different from the *Gal4* control (*for^{0}/for^{0}; {for^{pr3}-Gal4}/+*, $p = .06$) and the *UAS* control (*for^{0}/for^{0}; +/{UAS-for^{cDNA}}*, $p = .06$). D) The *pr4* experimental (*for^{0}/for^{0}; {for^{pr4}-Gal4}/{UAS-for^{cDNA}}*) was not significantly different from the *Gal4* control (*for^{0}/for^{0}; {for^{pr4}-Gal4}/+*, $p = 1.00$). Sample size: $n = 10$ extracts (of 10 pooled larvae) per genotype per plot. The boxplots show the mean with the whiskers displaying 1.5 times the interquartile range. For a rescue to be considered significant the *UAS/Gal4* treatment had to be significantly different than both of the *UAS* and the *Gal4* controls.

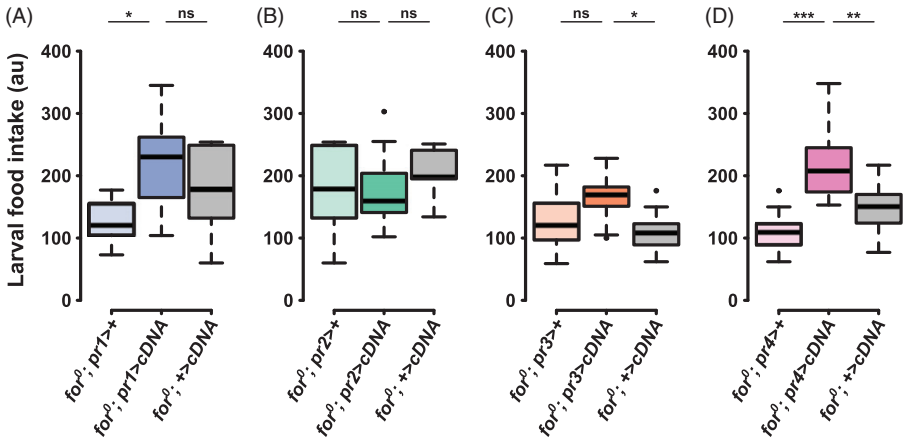

Figure 5. *for^{p4}-Gal4* rescues null larval food intake. (A) The *pr1* experimental (*for^{0}/for^{0}; {for^{pr1}-Gal4}/{UAS-for^{cDNA}}*) was not significantly different from the *UAS* control (*for^{0}/for^{0}; +/{UAS-for^{cDNA}}*, $p = .85$). (B) The *pr2* experimental (*for^{0}/for^{0}; {for^{pr2}-Gal4}/{UAS-for^{cDNA}}*) was not significantly different from the *Gal4* control (*for^{0}/for^{0}; {for^{pr2}-Gal4}/+*, $p = .87$) or the *UAS* control (*for^{0}/for^{0}; +/{UAS-for^{cDNA}}*, $p = .86$). (C) The *pr3* experimental (*for^{0}/for^{0}; {for^{pr3}-Gal4}/{UAS-for^{cDNA}}*) was not significantly different from the *Gal4* control (*for^{0}/for^{0}; {for^{pr3}-Gal4}/+*, $p = .18$). (D) The *pr4* experimental (*for^{0}/for^{0}; {for^{pr4}-Gal4}/{UAS-for^{cDNA}}*) was significantly different from the *Gal4* control (*for^{0}/for^{0}; {for^{pr4}-Gal4}/+*, $p = .00005$) and the *UAS* control (*for^{0}/for^{0}; +/{UAS-for^{cDNA}}*, $p = .006$). Sample size: $n = 10$ extracts (of 10 pooled larvae) per genotype per plot. The boxplots show the mean with the whiskers displaying 1.5 times the interquartile range. For a rescue to be considered significant the *UAS/Gal4* treatment had to be significantly different than both of the *UAS* and the *Gal4* controls.

rescue any of the larval phenotypes. In the nervous system it was expressed in midline glia which are crucial for midline axon guidance and nervous system morphogenesis (Jacobs, 2000). *for^{pr2}-Gal4* also expressed in the adult midgut precursors (AMPs) known to contain the intestinal stem cells and other support cells; during preparation for pupal development, these cells begin to increase in number to repopulate the midgut with adult cells (Jiang & Edgar, 2009). *for^{pr3}-Gal4* which bordered on significance to effect altered larval triglycerides had the widest expression pattern including the larval fat body, muscle, enterocytes, and the surface glia. The surface glia, made up of perineural and subperineurial glia, are important for blood–brain barrier activities (Edwards & Meinertzhagen, 2010). *for^{pr3}-Gal4* glial cells may be perineurial glia due to the size and number of cells (Stork, Bernardos, & Freeman, 2012). Interestingly, fat body, muscle, and enterocytes tissue systems have previously been shown to affect triglyceride levels (Lee, Bassel-Duby, & Olson, 2014; Song, Veenstra, & Perrimon, 2014). Allen *et al.*'s (2017) previous finding of increased triglyceride levels in *foraging* null larvae appears to contradict the findings of the present study where we found that *foraging* cDNA expressed using *for^{pr3}-Gal4* also increased triglyceride levels. One explanation for this discrepancy is that *foraging* functions antagonistically in different tissues to affect fat levels. This can be examined in the future by manipulating *foraging* using fat body, muscle or gut tissue specific drivers and measuring differences in larval triglyceride levels that arise from these manipulations. *for^{pr4}-Gal4* expression was sufficient to rescue larval food intake. It was restricted primarily to the optic lobes and discs, hindgut epithelia, and the spiracles. Relative to the other promoter driven *Gal4s for^{pr1}-Gal4* and *for^{pr4}-Gal4* were expressed in a restricted number of cells. This will facilitate future mapping of the specific

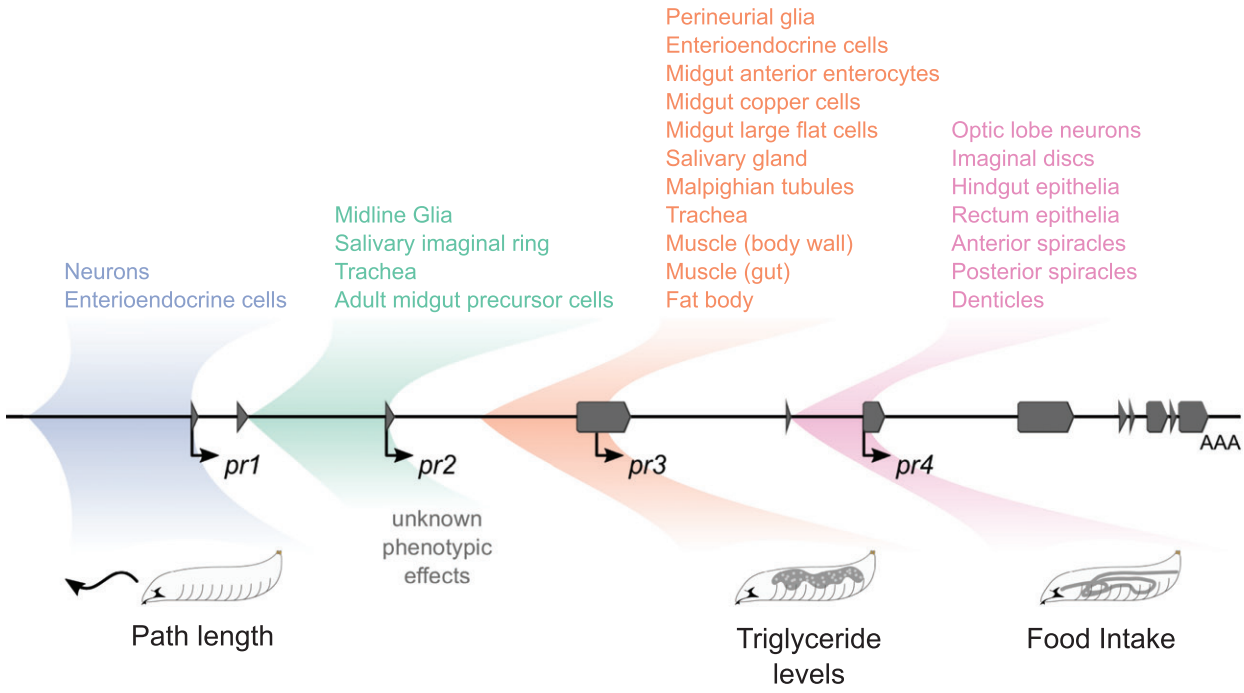

Figure 6. Summary of expression and phenotypic effects. A schematic of the *foraging* gene in the center with exons in grey and transcription start sites marked with arrows. The regions cloned in the *for*^{pr}*-Gal4*s are colored and shaded. The expression patterns seen in the *for*^{pr}*-Gal4*s are summarized above the locus. Depictions of the rescued phenotypes are shown below the locus.

cells responsible for each of the path length and food intake phenotype using intersectional methods such as by *Gal80* (Suster, Seugnet, Bate, & Sokolowski, 2004) and *Flp-out* (Bischof & Basler, 2008).

Recently, it was shown that products from *pr4* were responsible for affecting adult fly food intake and foraging behavior (Anreiter *et al.*, 2017). This suggests that larval and adult food intake may be regulated by the same *foraging* promoter across development. However, when comparing the results of Anreiter *et al.* (2017) to the present study, it becomes clear that larval foraging path length behavior and adult foraging behavior are likely controlled by different parts of the *foraging* gene, since *for*^{pr1}*-Gal4* and not *for*^{pr4}*-Gal4* rescued larval foraging behavior. Future experiments will determine which of these tissues or combination of tissues result in these larval and adult phenotypes (for further discussion see Anreiter & Sokolowski, 2018).

It is unlikely that the cloned fragments of *foraging* used in the present study to generate the *for*^{pr}*-Gal4*s encompass all of the DNA that regulates *foraging*. Significantly, however, these DNA fragments were sufficient for promoter specific rescues of the three larval phenotypes investigated here. The *for*^{pr}*-Gal4*s expression patterns reported in the present study direct us to the potential subsets of cells, and also to the DNA sequences that are important for each larval phenotype. These DNA regions also serve as pivotal regions of interest when looking for allelic differences in the *foraging* gene strains, such as in the rover and sitter allelic variants, as shown in Anreiter *et al.* (2017).

Overall, this work represents a significant advance in how the *foraging* gene elicits its phenotypic effects in the larva. The expression patterns reported here can be used to generate new hypotheses about where *foraging* is required for other of its pleiotropic phenotypes. For example, *foraging* has previously been implicated in nutrient absorption in larvae (Kaun, Chakaborty-Chatterjee, & Sokolowski, 2008) and gut function in adults (Urquhart-Cronish & Sokolowski, 2014). The enterocytes and enteroendocrine cells reported here are important for absorption and digestion of ingested nutrients and visceral muscle may affect peristalsis of nutrients through the gut. *foraging*'s orthologue in mice is known to function in smooth muscle (Hofmann, Feil, Kleppisch, & Schlossmann, 2006; Hofmann *et al.*, 2009; Lohmann, Vaandrager, Smolenski, Walter, & De Jonge, 1997) and it also affects gut passage time (Weber *et al.*, 2007). The *for*^{pr3}*-Gal4* also drove expression in the Malpighian tubules. The tubules are vital for ion balance in the hemolymph, and *foraging* has been previously characterized for influencing adult Malpighian tubule secretion rate (MacPherson *et al.*, 2004a, 2004b).

We successfully rescued the *foraging* null phenotypes of larval foraging path length, triglyceride levels (bordered on significance) and food intake by driving expression of *foraging* cDNA using individual promoters. This suggests that the expression captured by the *Gal4*s from the promoter fragments we cloned is likely representative of the expression of the *foraging* gene. An outstanding issue is whether the *for*^{pr}*-Gal4*s recapitulate native *foraging* expression. An antibody against *foraging* protein was previously published for immuno-histochemistry in the adult CNS (Belay *et al.*, 2007). Unfortunately, this antibody was unable to detect differences in staining between wild-type and *for*^{0} null mutant larvae. We were therefore unable to evaluate these *for*^{pr}*Gal4*s with our anti-FOR antibody. Microarrays on dissected tissue, RNA-seq on dissected tissue, and RNA-seq on sorted cells (from sources such as FlyAtlas, FlyAtlas2, modENCODE, and Flygut-seq) support our finding of *foraging* expression

in multiple tissues including the CNS, fat body, salivary glands, trachea, and the gut (Chintapalli *et al.*, 2007; Dutta *et al.*, 2015; Graveley *et al.*, 2011; Leader *et al.*, 2018). Future use of novel translation dependent protein trap techniques (Diao *et al.*, 2015; Venken *et al.*, 2011) may provide further transgenic methods for identifying the *foraging* gene's expression.

Conclusion

foraging's complex molecular structure contributes to the pleiotropy in larval feeding-related phenotypes. We rescued the larval path length, food intake, and triglyceride levels (bordered on significance) of the for^{0} null larvae by driving expression of a *UAS-*for^{cDNA} using individual for^{pr}*-Gal4*s. Each of the for^{pr}*-Gal4*s we generated had discrete, restricted expression patterns throughout the larva. The modularity of *foraging*'s molecular structure was also apparent in the phenotypic rescues. Our data support the hypothesis that *foraging*'s pleiotropy results from the individual contributions of its four *foraging* promoters. These results refine the spatial expression and the sub-regions of the gene responsible for *foraging*'s associated larval phenotypes. This study provides a road map for investigating other aspects of *foraging*'s pleiotropic effects in the larval and adult fly. This modular nature of *foraging*'s promoters and their different functions may have interesting implications for the evolutionary pressures acting on the locus. This differential regulation may serve as an adaptive escape from the constraints of pleiotropy (Des Marais & Rausher, 2008).

Acknowledgements

We would like to thank Jean-Christophe Billeter, and Joel Levine for guidance and advice as well as the Sokolowski Lab for helpful discussions. Megan Neville and Deniz Erezyilmaz for comments on the manuscript and two anonymous reviewers of this journal for helpful suggestions. Stocks obtained from the Bloomington Drosophila Stock Center (NIH P40OD018537) were used in this study.

Disclosure statement

No potential conflict of interest was reported by the authors.

Funding

This research was supported by grants from the Natural Sciences and Engineering Council of Canada (NSERC), the Canadian Institutes for Health Research (CIHR) and NIDDK grant 5R01DK70141-2 to MBS.

ORCID

I. Anreiter http://orcid.org/0000-0002-9563-0579
M. B. Sokolowski http://orcid.org/0000-0002-7462-8007

References

Allen, A.M., Anreiter, I., Neville, M.C., & Sokolowski, M.B. (2017). Feeding-related traits are affected by dosage of the *foraging* gene in *Drosophila melanogaster*. *Genetics*, *205*, 761–773. doi:10.1534/genetics.116.197939

Andersson, L., & Georges, M. (2004). Domestic-animal genomics: Deciphering the genetics of complex traits. *Nature Reviews Genetics*, *5*, 202–212. doi:10.1038/nrg1294

Anreiter, I., Vasquez, O.E., Allen, A.M., & Sokolowski, M.B. (2016). Foraging path-length protocol for *Drosophila melanogaster* larvae. *Journal of Visualized Experiments*, *110*, e53980. doi:10.3791/53980

Anreiter, I., Kramer, J.M., & Sokolowski, M.B. (2017). Epigenetic mechanisms modulate differences in *Drosophila* foraging behavior. *Proceedings of the National Academy of Sciences USA*, *114*, 12518–12523. doi:10.1073/pnas.1710770114

Anreiter, I., & Sokolowski, M.B. (2018). Deciphering pleiotropy: How complex genes regulate behavior. *Communicative & Integrative Biology*, e1447743. doi:10.1080/19420889.2018.1447743

Arredondo, J.J., Marco Ferreres, R., Maroto, M., Cripps, R.M., Marco, R., Bernstein, S.I., & Cervera, M. (2001). Control of *Drosophila paramyosin/miniparamyosin* gene expression. Differential regulatory mechanisms for muscle-specific transcription. *Journal of Biological Chemistry*, *276*, 8278–8287. doi:10.1074/jbc.M009302200

Ayoubi, T.A., & Van De Ven, W.J. (1996). Regulation of gene expression by alternative promoters. *FASEB Journal*, *10*, 453–460. doi:10.1096/fasebj.10.4.8647344

Barolo, S., Carver, L.A., & Posakony, J.W. (2000). GFP and β-galactosidase transformation vectors for promoter/enhancer analysis in *Drosophila*. *BioTechniques*, *29*, 726–732.

Belay, A.T., Scheiner, R., So, A. K.-C., Douglas, S.J., Chakaborty-Chatterjee, M., Levine, J.D., & Sokolowski, M.B. (2007). The *foraging* gene of *Drosophila melanogaster*: Spatial-expression analysis and sucrose responsiveness. *The Journal of Comparative Neurology*, *504*, 570–582. doi:10.1002/cne.21466

Billeter, J.-C., & Goodwin, S.F. (2004). Characterization of *Drosophila fruitless-gal4* transgenes reveals expression in male-specific *fruitless* neurons and innervation of male reproductive structures. *The Journal of Comparative Neurology*, *475*, 270–287. doi:10.1002/cne.20177

Bischof, J., & Basler, K. (2008). Recombinases and their use in gene activation, gene inactivation, and transgenesis. *Methods in Molecular Biology (Clifton, N.J.)*, *420*, 175–195. doi:10.1007/978-1-59745-583-1

Bischof, J., Maeda, R.K., Hediger, M., Karch, F., & Basler, K. (2007). An optimized transgenesis system for *Drosophila* using germ-line-specific phiC31 integrases. *Proceedings of the National Academy of Sciences USA*, *104*, 3312–3317. doi:10.1073/pnas.0611511104

Brand, A.H., & Perrimon, N. (1993). Targeted gene expression as a means of altering cell fates and generating dominant phenotypes. *Development*, *118*, 401–415.

Brenner, R., Thomas, T.O., Becker, M.N., & Atkinson, N.S. (1996). Tissue-specific expression of a Ca(2+)-activated K + channel is controlled by multiple upstream regulatory elements. *The Journal of Neuroscience*, *16*, 1827–1835. doi:10.1523/JNEUROSCI.16-05-01827.1996

Carroll, S.B. (2000). Endless forms: the evolution of gene regulation and morphological diversity. *Cell*, *101*, 577–580. doi:10.1016/S0092-8674(00)80868-5

Chintapalli, V.R., Wang, J., & Dow, J.A.T. (2007). Using FlyAtlas to identify better *Drosophila melanogaster* models of human disease. *Nature Genetics*, *39*, 715–720. doi:10.1038/ng2049

Des Marais, D.L., & Rausher, M.D. (2008). Escape from adaptive conflict after duplication in an anthocyanin pathway gene. *Nature*, *454*, 762–765. doi:10.1038/nature07092

Diao, F., Ironfield, H., Luan, H., Diao, F., Shropshire, W.C., Ewer, J., … White, B.H. (2015). Plug-and-play genetic access to *Drosophila* cell types using exchangeable exon cassettes. *Cell Reports*, *10*, 1410–1421. doi:10.1016/j.celrep.2015.01.059

Dubreuil, R.R. (2004). Copper cells and stomach acid secretion in the *Drosophila* midgut. *The International Journal of Biochemistry & Cell Biology*, *36*, 745–752.

Dutta, D., Dobson, A. J., Houtz, P. L., Gläßer, C., Revah, J., Korzelius, J., Patel, P. H., Edgar, B. A., Buchon, N. (2015). Regional cell-

specific transcriptome mapping reveals regulatory complexity in the adult Drosophila midgut. *Cell Rep*. *12*, 346–358.

Edwards, T.N., & Meinertzhagen, I.A. (2010). The functional organisation of glia in the adult brain of *Drosophila* and other insects. *Progress in Neurobiology*, *90*, 471–497. doi:10.1016/j.pneurobio.2010.01.001

Graveley, B.R., Brooks, A.N., Carlson, J.W., Duff, M.O., Landolin, J.M., Yang, L., … Celniker, S.E. (2011). The developmental transcriptome of *Drosophila melanogaster*. *Nature*, *471*, 473–479. doi:10.1038/nature09715

Groth, A.C., Fish, M., Nusse, R., & Calos, M.P. (2004). Construction of transgenic *Drosophila* by using the site-specific integrase from phage φC31. *Genetics*, *166*, 1775–1782. doi:10.1534/genetics.166.4.1775

Hodgkin, J. (1998). Seven types of pleiotropy. *International Journal of Developmental Biology*, *42*, 501–505.

Hofmann, F., Bernhard, D., Lukowski, R., & Weinmeister, P. (2009). *cGMP regulated protein kinases (cGK). cGMP: Generators, effectors and therapeutic implications* (pp. 137–162). Berlin, Heidelberg: Springer Berlin Heidelberg.

Hofmann, F., Feil, R., Kleppisch, T., & Schlossmann, J. (2006). Function of cGMP-dependent protein kinases as revealed by gene deletion. *Physiological Reviews*, *86*, 1–23. doi:10.1152/physrev.00015.2005

Hofmann, H.A. (2003). Functional genomics of neural and behavioral plasticity. *Journal of Neurobiology*, *54*, 272–282. doi:10.1002/neu.10172

Jacobs, J.R. (2000). The midline glia of Drosophila: A molecular genetic model for the developmental functions of glia. *Prog. Neurobiol*. *62*, 475–508.

Jiang, H., & Edgar, B.A. (2009). EGFR signalling regulates the proliferation of *Drosophila* adult midgut progenitors. *Development*, *136*, 483–493. doi:10.1242/dev.026955

Kalderon, D., & Rubin, G.M. (1989). cGMP-dependent protein kinase genes in *Drosophila*. *The Journal of Biological Chemistry*, *264*, 10738–10748.

Kaun, K.R., Chakaborty-Chatterjee, M., & Sokolowski, M.B. (2008). Natural variation in plasticity of glucose homeostasis and food intake. *The Journal of Experimental Biology*, *211*, 3160–3166. doi:10.1242/jeb.010124

Kaun, K.R., Riedl, C.A.L., Chakaborty-Chatterjee, M., Belay, A.T., Douglas, S.J., Gibbs, A.G., & Sokolowski, M.B. (2007). Natural variation in food acquisition mediated via a *Drosophila* cGMP-dependent protein kinase. *The Journal of Experimental Biology*, *210*, 3547–3558. doi:10.1242/jeb.006924

Kearse, M., Moir, R., Wilson, A., Stones-Havas, S., Cheung, M., Sturrock, S., … Drummond, A. (2012). Geneious basic: An integrated and extendable desktop software platform for the organization and analysis of sequence data. *Bioinformatics*, *28*, 1647–1649. doi:10.1093/bioinformatics/bts199

Leader, D. P., Krause, S. A., Pandit, A., Davies, S. A., Dow, J. A. T. (2018). FlyAtlas 2: A new version of the Drosophila melanogaster expression atlas with RNA-Seq, miRNA-Seq and sex-specific data. *Nucleic Acids Res*. *46*, D809–D815.

Lee, J.-H., Bassel-Duby, R., & Olson, E.N. (2014). Heart- and muscle-derived signaling system dependent on MED13 and Wingless controls obesity in *Drosophila*. *Proceedings of the National Academy of Sciences USA*, *111*, 9491–9496. doi:10.1073/pnas.1409427111

Lee, T., & Luo, L. (1999). Mosaic analysis with a repressible cell marker for studies of gene function in neuronal morphogenesis. *Neuron*, *22*, 451–461. doi:10.1016/S0896-6273(00)80701-1

Lehman, D.A., Patterson, B., Johnston, L.A., Balzer, T., Britton, J.S., Saint, R., & Edgar, B.A. (1999). *Cis*-regulatory elements of the mitotic regulator, *string/Cdc25*. *Development*, *126*, 1793–1803.

Lohmann, S.M., Vaandrager, A.B., Smolenski, A., Walter, U., & De Jonge, H.R. (1997). Distinct and specific functions of cGMP-dependent protein kinases. *Trends in Biochemical Sciences*, *22*, 307–312. doi:10.1016/S0968-0004(97)01086-4

MacPherson, M.R., Broderick, K.E., Graham, S., Day, J.P., Houslay, M.D., Dow, J.A.T., & Davies, S.A. (2004a). The dg2 (for) gene confers a renal phenotype in Drosophila by modulation of cGMP-specific phosphodiesterase. *J. Exp. Biol. 207*, 2769–2776.

MacPherson, M.R., Lohmann, S.M., and Davies, S.-A. (2004b). Analysis of Drosophila cGMP-dependent protein kinases and assessment of their in vivo roles by targeted expression in a renal transporting epithelium. *J. Biol. Chem. 279*, 40026–40034.

Markstein, M., Pitsouli, C., Villalta, C., Celniker, S.E., & Perrimon, N. (2008). Exploiting position effects and the *gypsy* retrovirus insulator to engineer precisely expressed transgenes. *Nature Genetics*, *40*, 476–483. doi:10.1038/ng.101

Murakami, R., & Shiotsuki, Y. (2001). Ultrastructure of the hindgut of *Drosophila* larvae, with special reference to the domains identified by specific gene expression patterns. *Journal of Morphology*, *248*, 144–150. doi:10.1002/jmor.1025

Okada, T., Sakai, T., Murata, T., Kako, K., Sakamoto, K., Ohtomi, M., … Ishida, N. (2001). Promoter analysis for daily expression of *Drosophila* timeless gene. *Biochemical and Biophysical Research Communications*, *283*, 577–582. doi:10.1006/bbrc.2001.4793

Ormö, M., Cubitt, A.B., Kallio, K., Gross, L.A., Tsien, R.Y., & Remington, S.J. (1996). Crystal structure of the *Aequorea victoria* green fluorescent protein. *Science*, *273*, 1392–1395. doi:10.1126/science.273.5280.1392

Osborne, K.A., Robichon, A., Burgess, E., Butland, S., Shaw, R.A., Coulthard, A., & Pereira, H.S. (1997). Natural behavior polymorphism due to a cGMP-dependent protein kinase of *Drosophila*. *Science*, *277*, 834–836. doi:10.1126/science.277.5327.834

Park, J.H., Helfrich-Förster, C., Lee, G., Liu, L., Rosbash, M., & Hall, J.C. (2000). Differential regulation of circadian pacemaker output by separate clock genes in *Drosophila*. *Proceedings of the National Academy of Science USA*, *97*, 3608–3613. doi:10.1073/pnas.97.7.3608

Pyeritz, R.E. (1989). Pleiotropy revisited: Molecular explanations of a classic concept. *American Journal of Medical Genetics*, *34*, 124–134. doi:10.1002/ajmg.1320340120

R Core Team (2018). R: A language and environment for statistical computing. R Foundation for Statistical Computing, Vienna, Austria. https://www.R-project.org/

Reaume, C.J., & Sokolowski, M.B. (2011). Conservation of gene function in behaviour. *Philosophical Transactions of the Royal Society of London B: Biological Sciences*, *366*, 2100. doi:10.1098/rstb.2011.0028

Schindelin, J., Arganda-Carreras, I., Frise, E., Kaynig, V., Longair, M., Pietzsch, T., … Cardona, A. (2012). Fiji: An open-source platform for biological-image analysis. *Nature Methods*, *9*, 676–682. doi:10.1038/nmeth.2019

Schlossmann, J., & Desch, M. (2009). *cGK substrates. cGMP: Generators, effectors and therapeutic implications* (pp. 163–193). Berlin, Heidelberg: Springer Berlin Heidelberg.

Smith, J.A., Francis, S.H., Walsh, K.A., Kumar, S., & Corbin, J.D. (1996). Autophosphorylation of type Ibeta cGMP-dependent protein kinase increases basal catalytic activity and enhances allosteric activation by cGMP or cAMP. *The Journal of Biological Chemistry*, *271*, 20756–20762. doi:10.1074/jbc.271.34.20756

Song, W., Veenstra, J.A., & Perrimon, N. (2014). Control of lipid metabolism by *tachykinin* in *Drosophila*. *Cell Reports*, *9*, 40–47. doi:10.1016/j.celrep.2014.08.060

Stork, T., Bernardos, R., & Freeman, M.R. (2012). Analysis of glial cell development and function in *Drosophila*. *Cold Spring Harbor Protocols*, *2012*, 1–17.

Suster, M.L., Seugnet, L., Bate, M., & Sokolowski, M.B. (2004). Refining GAL4-driven transgene expression in *Drosophila* with a GAL80 enhancer-trap. *Genesis*, *39*, 240–245. doi:10.1002/gene.20051

Thomas, T., Wang, B., Brenner, R., & Atkinson, N.S. (1997). Novel embryonic regulation of Ca(2+)-activated K + channel expression in *Drosophila*. *Invertebrate Neuroscience*, *2*, 283–291. doi:10.1007/BF02211941

Urquhart-Cronish, M., & Sokolowski, M.B. (2014). Gene-environment interplay in *Drosophila* melanogaster: Chronic nutritional deprivation in larval life affects adult fecal output. *Journal of Insect Physiology*, *69*, 95–100. doi:10.1016/j.jinsphys.2014.06.001

Veenstra, J.A. (2009). Peptidergic paracrine and endocrine cells in the midgut of the fruit fly maggot. *Cell and Tissue Research*, *336*, 309–323. doi:10.1007/s00441-009-0769-y

Venken, K.J.T., Schulze, K.L., Haelterman, N.A., Pan, H., He, Y., Evans-Holm, M., … Bellen, H.J. (2011). MiMIC: A highly versatile transposon insertion resource for engineering *Drosophila melanogaster* genes. *Nature Methods*, *8*, 737–743. doi:10.1038/nmeth.1662

Weber, S., Bernhard, D., Lukowski, R., Weinmeister, P., Worner, R., Wegener, J.W., … Feil, R. (2007). Rescue of cGMP kinase I knockout mice by smooth muscle specific expression of either isozyme. *Circulation Research*, *101*, 1096–1103. doi:10.1161/CIRCRESAHA.107.154351